

November 24, 2003

John Vandecar
Senior Editor, Nature
968 National Press Building
Washington DC 20045-1938, USA

Re: Revision to *Cooling history of the Pacific lithosphere*, by M.H. Ritzwoller, N.M. Shapiro, and S. Zhong

Dear John,

As you may recall, the main results and conclusions reached in this paper are as follows:

1. Surface wave speeds for particular periods and wave types flatten in the Central Pacific, particularly in the age range from about 70 to 100 Ma.
2. The principal consequence is that velocity and temperature are approximately constant in this age range at depths ranging from about 70 to 150 km.
3. We interpret this feature to indicate a punctuated cooling history of the Pacific lithosphere in which the average cooling of the lithosphere brackets a period of reheating. This reheating occurs from about 70 to 100 Ma on average at depths ranging from about 70 to 150 km dominantly.
4. We point to thermal boundary layer instabilities (TBI), elsewhere sometimes called small-scale sub-lithospheric convection, as a potential contributing cause of the punctuated cooling history of the Pacific lithosphere.

These results are based on a number of largely technical innovations, which include:

1. A large new data set of broad-band surface wave speeds, particularly group velocities at periods shorter than have been applied on large-scales previously. This significantly improves the vertical resolution of the model in the uppermost mantle.
2. A tomographic method that includes modeling the spatial extent of the surface wave sensitivity kernels that produces more reliable amplitudes and gives a better estimate of intrinsic lateral resolution.
3. A Monte-Carlo inversion that allows us to estimate model uncertainties and interpret only those features that are significant.
4. The imposition of physical constraints on the inversion through a thermal model that is the basis for the temperature parameterization of the model.
5. A detailed comparison with a simple reference model: the half-space cooling (HSC) model.
6. A general comparison with a 3-D geodynamical simulation of TBI.

Jeannot Trampert and Geoff Davies delivered thought provoking reviews. They appear to understand the methods that we have employed and our arguments well. Jeannot questions the veracity of the seismic model, as he suspects that the main seismological signal that we interpret,

the reduction of surface wave velocities and shear velocities in the Central Pacific relative to the predictions of a diffusively cooling half-space, results from bias caused by azimuthal anisotropy. Geoff Davies suggests that the thermal model on which the temperature parameterization is based biases the inferred temperature and seismic models toward our main conclusions. These are plausible concerns which, if correct, suggest that the conclusions we have drawn may be wrong.

In a detailed response to Jeannot below, we demonstrate that azimuthal anisotropy is not causing the seismic signal that we interpret. We also argue that our model is not obviously at variance with seafloor topography as Jeannot also suggests. Geoff's concerns are somewhat less straightforward and are, therefore, more difficult to set aside definitively. We show, however, that the signals that we interpret do not depend on the thermal model that is the basis for our temperature parameterization. Our conclusions can also be reached from the model that results from our seismic parameterization. Geoff also suggests that presenting our results as a function of lithospheric age is wrong-headed or at least misleading. He contends that geographical location is a better independent variable. At his suggestion, we also present a plot below (Fig. 9) showing how the velocities in the model change parallel to isochrons. The main signals that we interpret remain readily apparent when the results are presented in this way, too. Geography is, indeed, the right explanatory variable for relatively small-scale heterogeneities (several thousand km), but the structure we interpret extends north-south across nearly the entire Pacific in a crescent-shaped feature that is best explained by the age of the lithosphere rather than its proximity to hot-spot plumes, deeper mantle up-wellings, etc.

Here is a summary of our responses to the reviewers' principal comments and how we have revised the paper.

1. In response to Jeannot's concern about potential bias caused by azimuthal anisotropy, we added a comment that the principal results of the paper are robust to the simultaneous estimation of azimuthal anisotropy. Figures 1 - fig:5 below demonstrate the robustness of our interpretation to the specification of azimuthal anisotropy in the inversion. Because the prediction of topography potentially is a hornet's nest, we have not added any discussion of it in the paper.
2. Geoff Davies requests that there be greater emphasis on the seismological results in the paper. In response, we introduced a new Figure 1 to the paper which shows several surface wave dispersion maps, how they relate to predictions from the HSC model, and how they vary with lithospheric age. (The original four figures have been merged into three figures in the revised text. We've removed parts of the original figures to be able to do this.) The signal that we interpret in the seismic and temperature models, the flattening of seismic speeds and temperatures in the lithosphere between 70 and 100 Ma, is apparent in the dispersion maps as a crescent shaped anomaly that follows more or less between the 70 and 100 Ma isochrons. He also suggests that we replace the seismic model based on the temperature parameterization with the model that derives from the seismic parameterization. This is a helpful suggestion that we considered carefully, but have chosen not to follow because we believe that the seismic model obtained with the thermal parameterization is better than that obtained with the seismic parameterization. We argue this point below in the detailed response to Geoff.
3. Geoff believes that presenting our results systematically as a function of lithospheric age is inappropriate. We provide further evidence (Fig. 9 below) that age is the natural explanatory variable for the anomalies that we discuss in this paper. There is also structural variability

in the Pacific lithosphere and asthenosphere that would be best explained by geography, but these signals are not the subject of this paper.

4. Geoff argues that the thermal model that is the basis for our temperature parameterization biases our conclusions and suggests that we remove plots of the “apparent thermal age” from the paper as they add little to the discussion and are potentially misleading. We show below (Figs. 7-8) that our main inferences derive also from the model based on the seismic parameterization, and argue that estimates of the thermal age of the lithosphere are a very effective way of summarizing lithospheric structure in simple maps. As Geoff points out, thermal age can be considered as a proxy for lithospheric thickness which can be estimated from it, but lithospheric thickness is not a variable in our thermal parameterization.
5. Geoff is also skeptical of the role of thermal boundary instabilities (TBI) in affecting the temperature conditions in the Central Pacific. He may be more amenable to thermal plumes generating heating events in the Central Pacific. We have revised the paper to make plumes somewhat more prominent, as well as other physical processes – particularly to explain the isochronous variance in the model. We have modified our discussion to make it clearer that TBI may be most important to explain the mean age trend of surface wave dispersion and 3-D seismic and temperature structure, whereas other processes are needed to explain the geographical variability of these variables. Nevertheless, we argue below based on the figure suggested by Geoff (Fig. 9) that lithospheric age is the simplest variable to invoke to explain our observations. As TBI depend intimately on age, invoking them in the name of explaining our observations is natural.

Sincerely,
Michael H. Ritzwoller
Nikolai M. Shapiro
Shijie Zhong

Detailed Response to Referee 1 (Jeannot Trampert)

Jeannot Trampert raises two principal concerns that we respond to here in some detail.

A.

Jeannot’s first concern relates to the veracity of the seismic model that we present. His evidence is summarized in Figure 1 in which he shows that two 40 sec Rayleigh wave dispersion maps constructed for isotropic velocity alone (without explicitly specifying azimuthal anisotropy simultaneously in the inversion) display a dip between 75 and 115 Ma that he calls a “kink” in the velocity versus age curve. Smoother isotropic maps or maps constructed simultaneously with azimuthal anisotropy do not display the dip. He argues that these kinks in the Central Pacific are caused by spurious “blobs” that appear because the inverse problem is not fully specified. He suggests that the flattening of the velocity versus age curve that we observe is caused not by the arrested cooling of the lithosphere in the Central Pacific as we argue, but by a bias introduced due to the fact that we have failed to account for azimuthal anisotropy in the tomographic inversion.

Jeannot is right that azimuthal anisotropy and the nature and extent of damping do change the details in the tomographic maps. This is one of the reasons we have concentrated our discussion on age averages in the paper, which are more robust to these changes, rather than interpreting the details in the maps. The flattening of the dispersion curves in the Central Pacific, however, is more

robust than Jeannot believes. We show our evidence for this conclusion here and conjecture below why Jeannot’s results differ from ours.

Figure 2a-c shows three 50 sec Rayleigh wave phase velocity maps. About 1/3 of the data are Jeannot’s measurements and about 2/3 come from the Harvard group. Thus, they’re not our measurements. We’ll summarize results for our measurements of group velocities shortly. Figure 2a is a moderately damped phase speed map (similar to the one used in the model discussed in the paper) and has been constructed without azimuthal anisotropy. Figure 2b shows the isotropic map that is damped similarly to that in to Figure 2a, but azimuthal anisotropy has been estimated simultaneously. The specification of azimuthal anisotropy does change the amplitude of isotropic features as seen, for example, by a diminishment of amplitude of the negative anomaly south of Hawaii. To a lesser extent the geometry is also affected. The map of azimuthal anisotropy estimated simultaneously with the isotropic map in Figure 2b is shown in Figure 3. The black and red lines and “error bars” in Figure 2d show, however, that both maps display a flattening of velocity versus age between 70 and 100 Ma. Note that in the paper we interpret a “flattening” of the velocity versus age curves rather than a “kink” and interpret the velocity versus age curves in terms of a flattening of the isotherms in this age range.

Figure 2c shows a smoother phase velocity map estimated with stronger isotropic damping, but without azimuthal anisotropy. The inversion is identical to that in Figure 2a, but the damping is stronger. The green line in Figure 2d shows that in this case, the flattening of the dispersion curve is attenuated.

Similar results are shown for the 100 sec Rayleigh wave group velocity in Figures 4 and 5. These maps are derived from our measurements. Even though group and phase velocity sensitivity kernels are somewhat different from one another, the maps in Figure 2 are very similar to those in Figure 4. In the case of the group velocity maps, the sensitivity to the specification of azimuthal anisotropy is somewhat greater than for phase velocity, but the principal age dependent features of the maps remain largely unchanged.

What the examples shown in Figures 2 - 5 demonstrate is that the inference of the flattening of the velocity versus age curves (and hence the isotherms in the Central Pacific that emerge in our 3-D model) is not caused by bias of the isotropic maps due to azimuthal anisotropy. In fact, the shape of the velocity versus age curve is controlled much more by isotropic damping than by the presence or absence of azimuthal anisotropy in the inversion. We have investigated this in some detail and find that as long as the resolution of an isotropic map is better than 1200 km, one is able to observe the flattening of the velocity versus age curve between 70 and 100 Ma. (Resolution is defined here as twice the standard deviation of a 2-D Gaussian fit to the resolution surface.)

So, what is the cause of the Jeannot’s results in Figure 1 if it is not bias caused by azimuthal anisotropy? We can only speculate, but Jeannot does his inversions differently than we do. When we add azimuthal anisotropy in the inversion, we attempt to find a relative damping of the isotropic and anisotropic maps that holds the isotropic resolution approximately constant. Jeannot does not take this approach, and prefers to choose an effective relative damping that holds the trace of the resolution matrix approximately constant. The effect is that when he introduces azimuthal anisotropy, the resolving power for isotropic structure degrades. We speculate, therefore, that Jeannot is not seeing evidence for bias due to azimuthal anisotropy as much as he is seeing the effect of producing a smoother isotropic map when he estimates azimuthal anisotropy simultaneously.

We cannot be certain that we have succeeded to illuminate the meaning of Jeannot’s results, but are confident that the seismological results that we present and the inferences drawn from them are not dependent on the neglect of azimuthal anisotropy in our inversions. We plan in our next global model for the isotropic maps to be constructed jointly with azimuthal anisotropy to lay concerns such as Jeannot’s to rest for good. This will not, however, affect the results we present in

this paper.

B.

Jeannot also is concerned that our model is in some way incompatible with observations of seafloor topography. This is a difficult issue that was the subject of one of our student's projects recently. (Ritzwoller, M.H., N.M. Shapiro, S. Zhong, W. Landuyt, and G.M. Leahy, Lithospheric thickness and seafloor topography inferred from a global seismic, EOS, Transactions Amer. Geophys. Un., 82(47), Fall meeting, 2001.) We have chosen not to address this issue in this paper as it may raise more questions than it answers. Our belief is that our model is consistent with seafloor topography to the extent that uppermost mantle temperatures may affect seafloor topography, but this mechanism may be unclear. For example, if high lithospheric temperature is caused by a mantle plume you would expect elevated seafloor, but if the causative agent is thermal boundary instabilities (small-scale convection) then seafloor may not be elevated as small-scale convection not only heats the lithosphere it cools the asthenosphere. The net affect on topography may be very small. In the long run, the relation between seafloor topography and mantle temperatures may help to unravel the cause of elevated seafloor topography, but we believe it is too early for this now.

Figure 6 shows some preliminary comparisons between observed seafloor topography and topography predicted from our model based on the student project. For the comparison to be meaningful, first, you need to reduce seafloor topography in a way that will accentuate the part of topography that would result from mantle temperatures. Numerous physical factors affect seafloor topography, including mantle temperature expressed in topography by isostatic compensation, sediments, crustal thickness, dynamical topography emanating from the deeper mantle, and volcanic edifices especially in large igneous provinces (LIPs). We have reduced seafloor topography by removing sediments, allowing the crust to rebound and segregating regions where there is reason to believe that the crust is thick or that are part of LIPs. We have done this only in a preliminary way and the results remain unpublished, but an example is shown in Figure 6 for several profiles across the Pacific. The topography predicted from the mantle model assumes isostatic compensation with a depth of compensation of 150 km. Figure 6b-d shows three profiles: $A - A'$, $B - B'$, and $C - C'$. Agreement is generally fairly good, except near LIPs.

Results aggregated versus lithospheric age are shown in Figure 6e. The general shape of the observed (reduced) and predicted topography are actually fairly similar. They both flatten at about 70 Ma and begin to deepen somewhat between 100 - 110 Ma on average. The removal of the LIP regions from consideration and stripping off the sediments increases observed seafloor depths in the old Pacific, bringing them into closer agreement with the predictions from our seismic model.

A comparison between seafloor topography and our seismic model is, therefore, beyond the scope of the present paper. We wish to point out here, however, that we do not believe that there is an obvious disagreement between seafloor topography and our seismic model, as Jeannot appears to believe.

Detailed Response to Referee 2 (Geoff Davies)

Geoff Davies raises two principal concerns that we now address.

A.

Geoff is generally skeptical of the application of the thermal model that is the basis for our temperature parameterization. He argues that it is incapable of accurately representing the temperature

signature of heating caused by plumes or TBI and worries that its use biases our results. As a consequence, he suggests that we abandon it in favor of the seismic parameterization. He also suggests that we specifically remove mention of “apparent thermal age” as it is misleading and adds little to the discussion.

There are several independent issues here.

First, the thermal model that is the basis for our temperature parameterization may be more general than Geoff realizes. Although lithospheric temperatures are represented with an error function (with free variable τ , apparent thermal age), a transition region knits it together with an adiabatic mantle beneath (with free variable T_p , potential temperature). We find that we can fit the seismic data very well with this pair of unknowns (τ, T_p). It is true that the resulting temperature profile is monotonically increasing with depth and, therefore, is not able to represent the effect of thermal plumes or TBI perfectly, as they will impart a shallow temperature minimum near the base of the lithosphere. The parameterization will not quite get the temperature profile right, but will mark the existence of a temperature minimum by reducing apparent thermal age, which can be thought of as proxy for lithospheric thickness or average lithospheric structure. We have used our thermal model to parameterize the temperature structure of Shijie Zhong’s 3-D simulation of TBI and have found that it reproduces temperatures fairly accurately. More importantly, the effect of TBI clearly emerges in a reduction of apparent thermal age.

Second, the use of the thermal model does not bias our principal results, although certainly any parameterization that one chooses will imprint itself in at least the details of the resulting model. We see subtle differences between the 3-D shear velocity and temperature models that result from the seismic and temperature parameterizations, but the main features that we interpret in this paper are the same and the conclusions we draw are robust relative to the choice of parameterization. Figures 7 and 8 below that emerge from the seismic parameterization are in all principal features indistinguishable from similar figures produced with the temperature parameterization, Figures 3 and 4 of the paper. There is, therefore, no compelling reason to replace the results from the thermal parameterization with the seismic parameterization. We actually prefer the temperature parameterization because the inferred mantle structure is more robust to uncertainties in crustal properties, particularly crustal thickness. Having more degrees of freedom than the temperature parameterization, the seismic parameterization is more prone to degradation due to our ignorance of crustal thickness.

Third, Geoff suggests that we delete images of the apparent thermal age. It is not true that τ , shown in Figure 4 of the paper, provides no information not contained in Figure 3 of the paper. τ is the single variable that represents lithospheric structure. One map of τ provides all of the information we have about the lithosphere. It effectively summarizes an incredible amount of information. Figure 3, in contrast, presents a plot of shear velocity at only one depth, 100 km, which in the central and western Pacific is in the lithosphere but in the eastern Pacific is beneath it. One might argue that only temperature or shear velocity results should be presented, as they are interconvertible. There are, however, two target audiences: seismologists and geodynamicists. The latter group probably would prefer to see temperatures and the former group shear wave speeds. In addition, shear velocity has the feature of standing close to the data, but temperature is the primitive variable that we directly estimate. Finally, the observed apparent thermal age can be compared readily to the apparent thermal age of the TBI simulation, as we have done in Figure 4d of the revised paper. For these reasons, we have chosen to retain the plots of apparent thermal age in the paper.

B.

Geoff questioned whether or not the deviations from the HSC model that we observe are predominately a function of age (e.g., his comments on the deviations in the western Pacific versus those of the east Pacific). He suggested that geography may be a better explanatory variable (e.g., proximity to plumes) and recommended that we compare profiles parallel to and normal to isochrons. This is a very helpful suggestion. We constructed Figure 9, which is very similar to what he suggested.

Figure 9 compares isochronous (nearly north-south) profiles of shear velocity at 100 km depth, to the prediction from the HSC model. The principal observed feature is that while the shear wave speeds along 20 and 60 Ma profiles on average are well predicted by the HSC model, the wave speeds do not increase from about 60 to 100 Ma. Note that the 100 Ma profile nowhere touches the HSC prediction for 100 Ma lithosphere. Thus, the discrepancy between observed and HSC predicted shear wave speeds extends north-south across the entire Pacific. In fact, it follows the 70-100 Ma region tracing a crescent shaped feature across the Pacific. In our view, this is a remarkable feature that demands interpretation in terms of the age of the lithosphere. Figure 9 also shows that the shear wave speeds deviate from the HSC model more strongly between ages of 70 and 100 Ma (the central Pacific) than that in younger region (the east Pacific).

It is because of this fact that we draw the reader's attention to TBI. It is even more interesting, in our view, that with the right rheology TBI can set on at about 70 Ma, largely stabilize by about 100 Ma, and elevate temperatures and reduce shear velocities in the depth range that we observe (70-150 km). We believe that this is compelling evidence for the existence of TBI as a principal dynamical agent that affects the thermal structure of the lithosphere in the central and old Pacific.

We point out that variations of shear speeds with latitude at constant age are apparent with typical length scales of 1000-3000 km for all the profiles in Figure 9 including the 20 and 60 Ma profiles. In particular, the 60 Ma profile shows a hemispherical variations; the northern hemisphere at this depth is faster than the southern hemisphere. These are interesting features that require physics (e.g., plumes, variations in conditions of formation) other than TBI to explain in most cases. This is not the subject of this paper, however.

Rayleigh 40 s

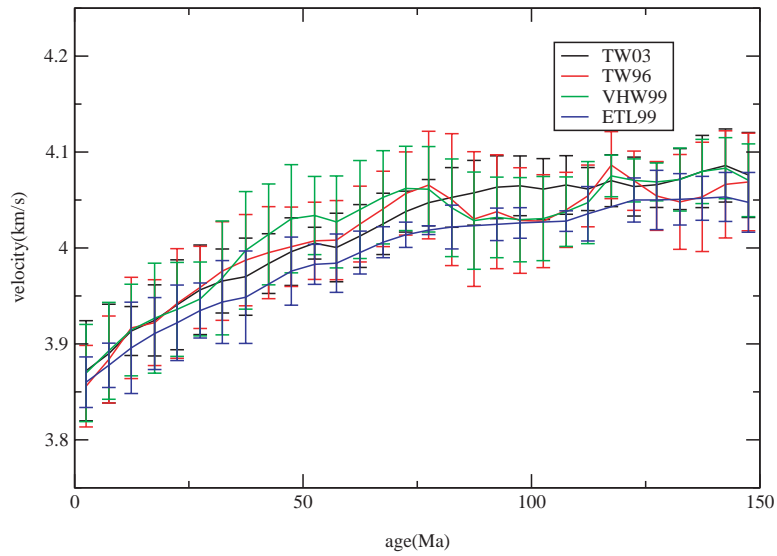


Figure 1: Dispersion results compiled by Trampert for the 40 sec Rayleigh wave. Trampert's early result (red line) and that of Van Heijst (green line) show a dip between 75 and 120 Ma which Trampert attributes to the biasing effect of azimuthal anisotropy, as these maps were constructed for isotropic velocity alone. The black line is Trampert's later results, where anisotropy is included in the inversion. The dip in the Central Pacific is not seen. The blue line is the result from Ekstrom et al. which does not include anisotropy in the inversion but also does not show the dip presumably because the map is highly damped.

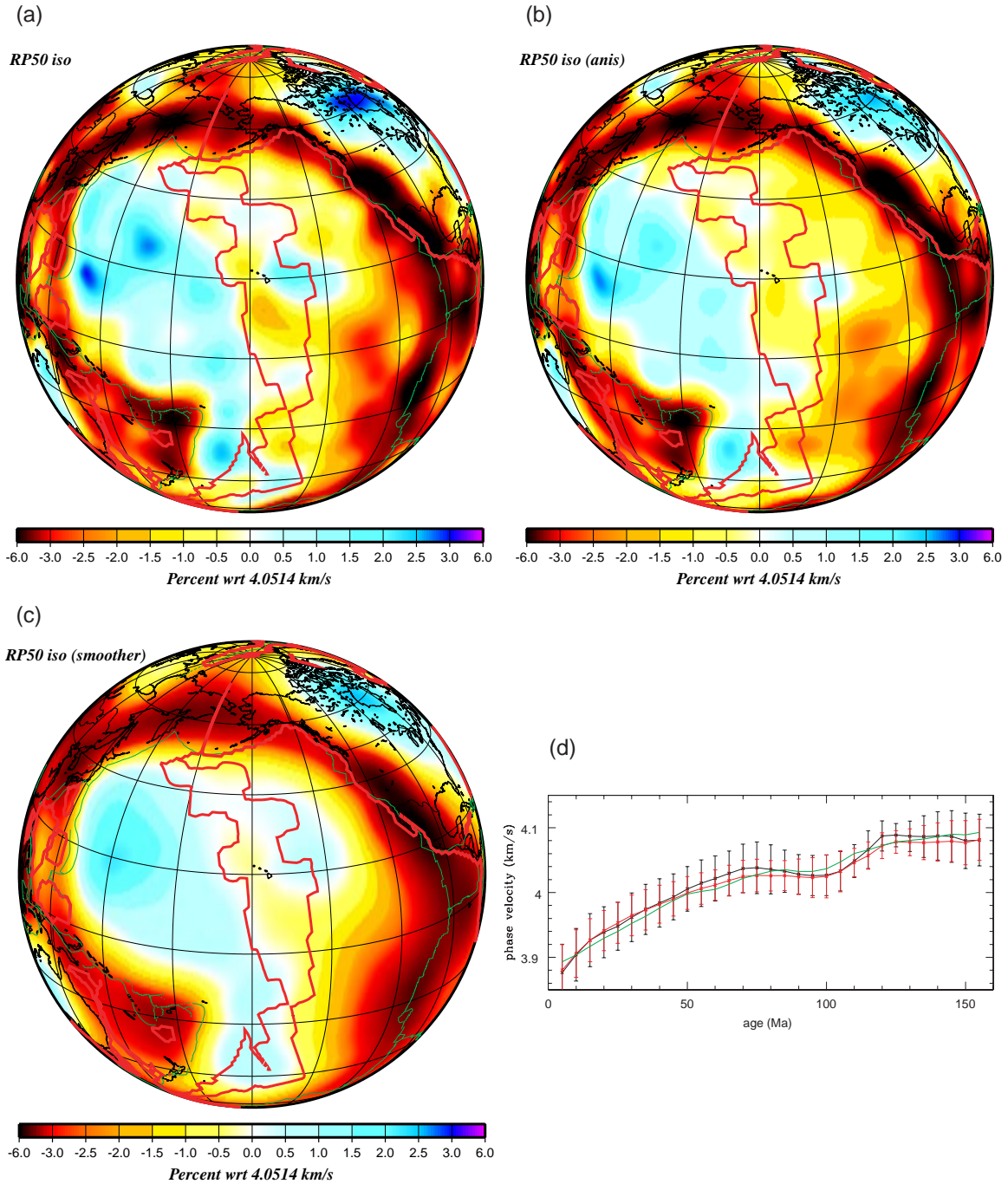


Figure 2: 50 sec Rayleigh wave phase velocity maps demonstrating the effect of jointly estimating azimuthal anisotropy and changing damping. (a) Only isotropic structure is specified in the inversion. This map is moderately damped, similar to the map used to construct the 3-D model discussed in the manuscript. (b) Azimuthal anisotropy is included in the inversion but isotropic damping (and therefore resolution) is kept approximately the same as in (a). The anisotropic map is shown in Figure 3. (c) An isotropic map that is more damped than (a), and azimuthal anisotropy has not been estimated simultaneously. Velocity variations in (a)-(c) are percent perturbations. Red lines in the Central Pacific mark the 70 and 110 Ma isochrons. (d) Average phase velocity versus age for the three maps in (a) - (c): black line and 1σ variation from (a), red line and 1σ variation from (b), green line from (c). Velocity flattens in the Central Pacific even when azimuthal anisotropy is included in the inversion, but does not flatten appreciably for the highly damped map even though azimuthal anisotropy is not estimated simultaneously.

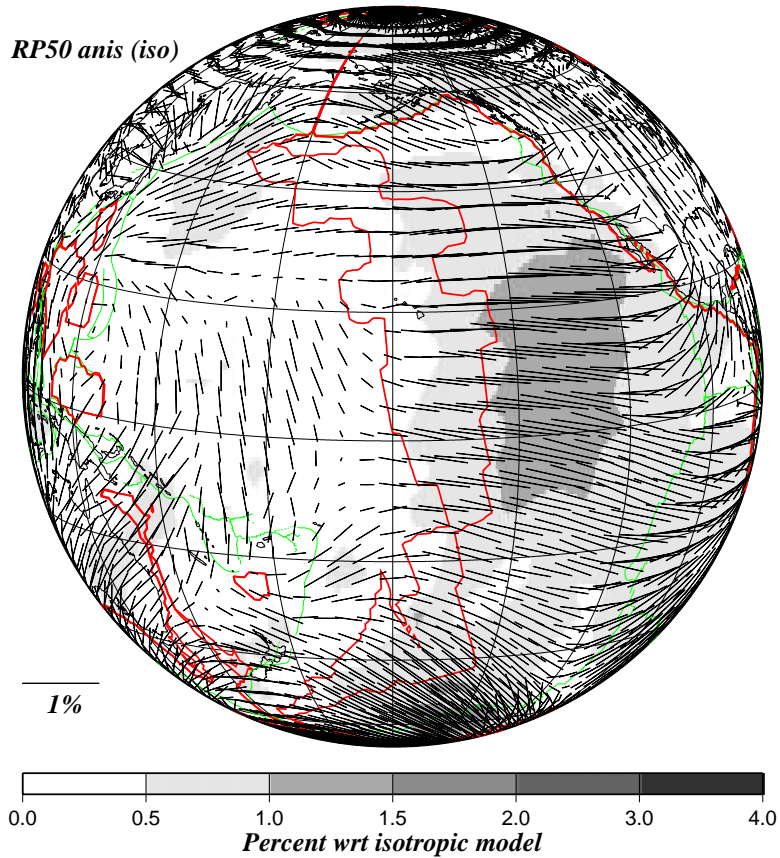


Figure 3: Azimuthal anisotropy (50 sec Rayleigh wave phase velocity) estimated simultaneously with the isotropic map shown in Figure 2b. Grey shades indicate the strength of anisotropy (maximizing at more than 1%) and vectors show the 2Ψ fast axis directions with length scaling with amplitude. Red lines in the Central Pacific identify 70 and 110 Ma lithosphere.

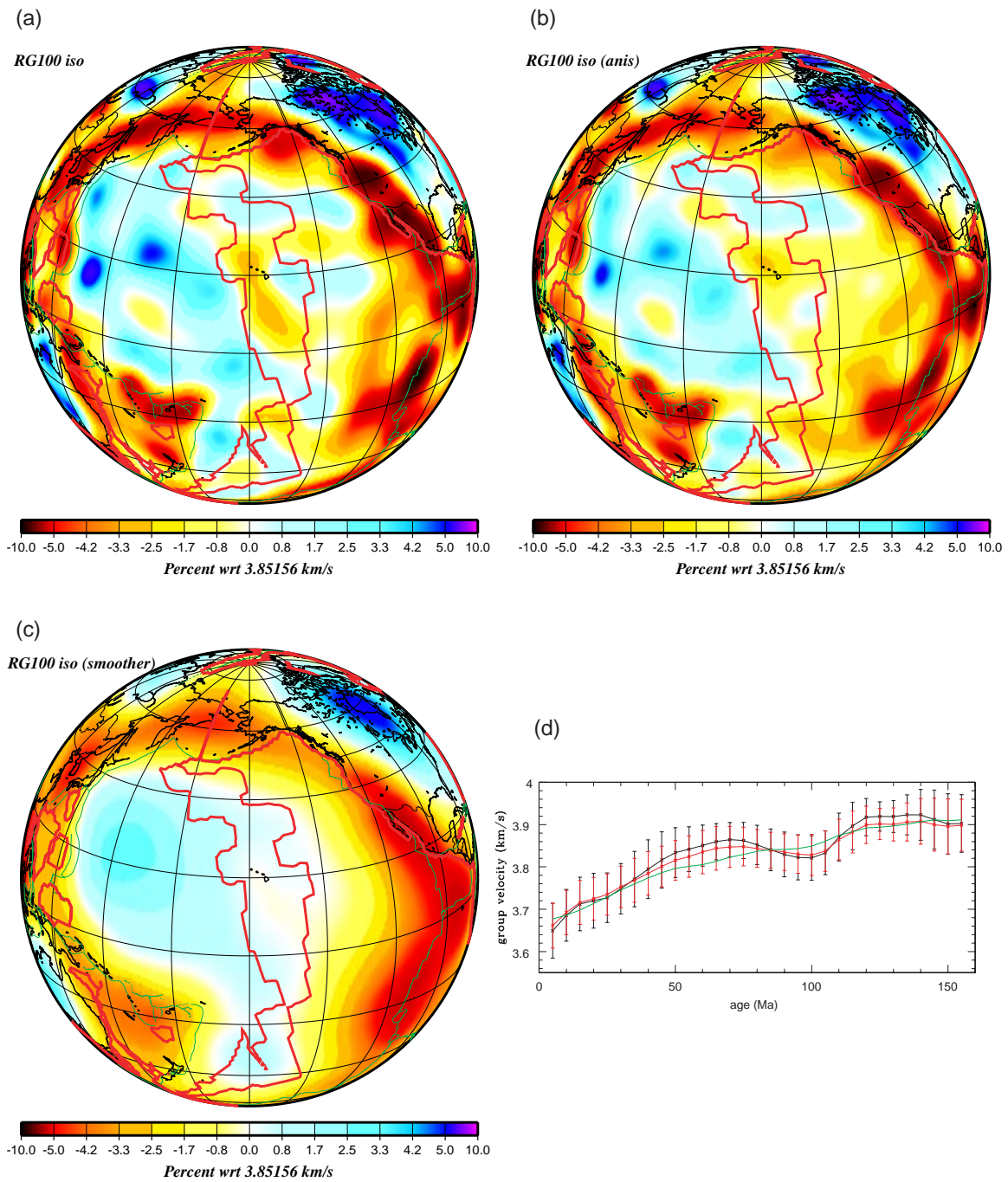


Figure 4: 100 sec Rayleigh wave group velocity maps, demonstrating similar results seen for the phase velocity maps in Figure 2. Azimuthal anisotropy estimated simultaneously with the map in (b) is shown in Figure 5. Damping of the isotropic structures controls the flattening of the curves been 70 and 100 Ma seen in (d) here and in Figure 2d much more strongly than the simultaneous inversion of azimuthal anisotropy.

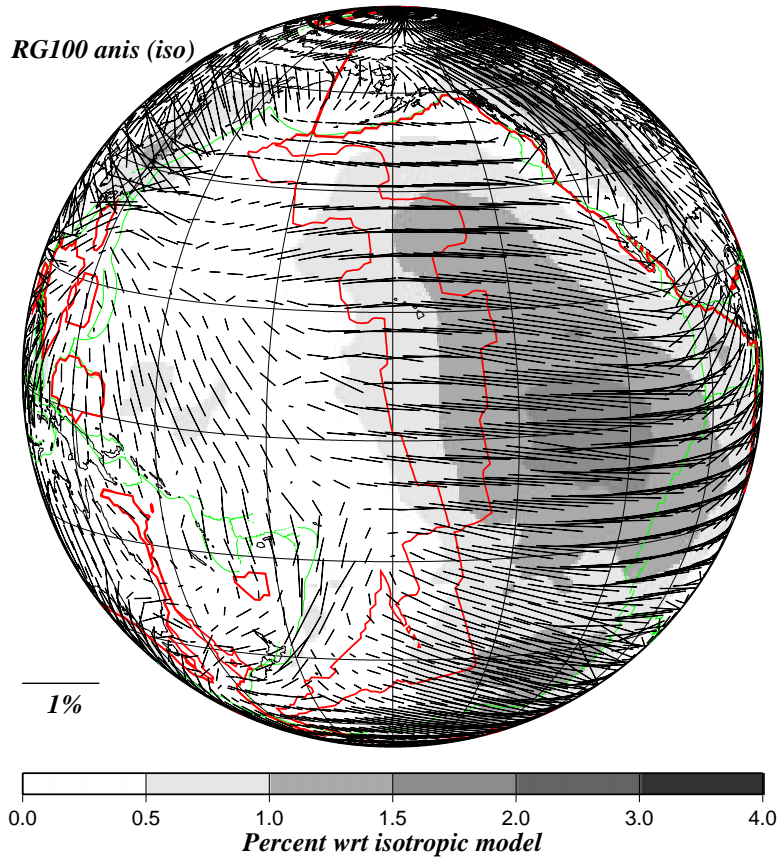


Figure 5: Azimuthal anisotropy (100 sec Rayleigh wave group velocity) estimated simultaneously with the isotropic map shown in Figure 4b, similar to Figure 3. Anisotropy maximizes at about 2% in this model.

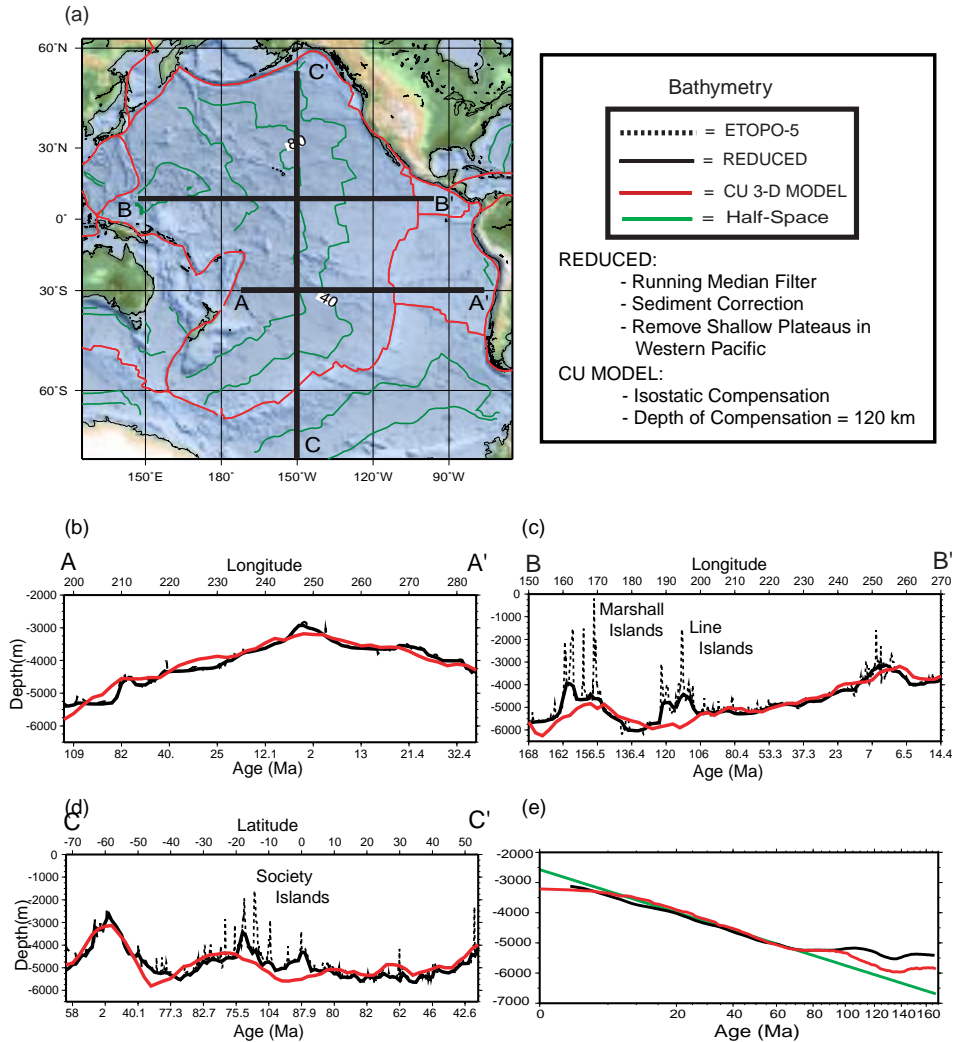


Figure 6: Comparison between observed topography and topography predicted from a seismic model. Observed topography is reduced by applying a running median filter to remove spiky features, removing sediments and allowing the crust to rebound isostatically, and segregating Large Igneous Provinces (LIPs) and oceanic plateaus. (a) Location of three profiles $A - A'$, $B - B'$, and $C - C'$. (b) Observed (reduced) and predicted topography along profile $A - A'$. The black line is observed and the red line is predicted topography. (c) and (d) Similar to (b), but for profiles $B - B'$ and $C - C'$. Discrepancy is greatest near Large Igneous Provinces (LIPs). (d) Comparison between reduced observed topography with topography predicted from our 3-D model and the half-space cooling model. The black line is observed reduced topography, the red line is predicted from the 3-D seismic model, and the green line is the half-space cooling model.

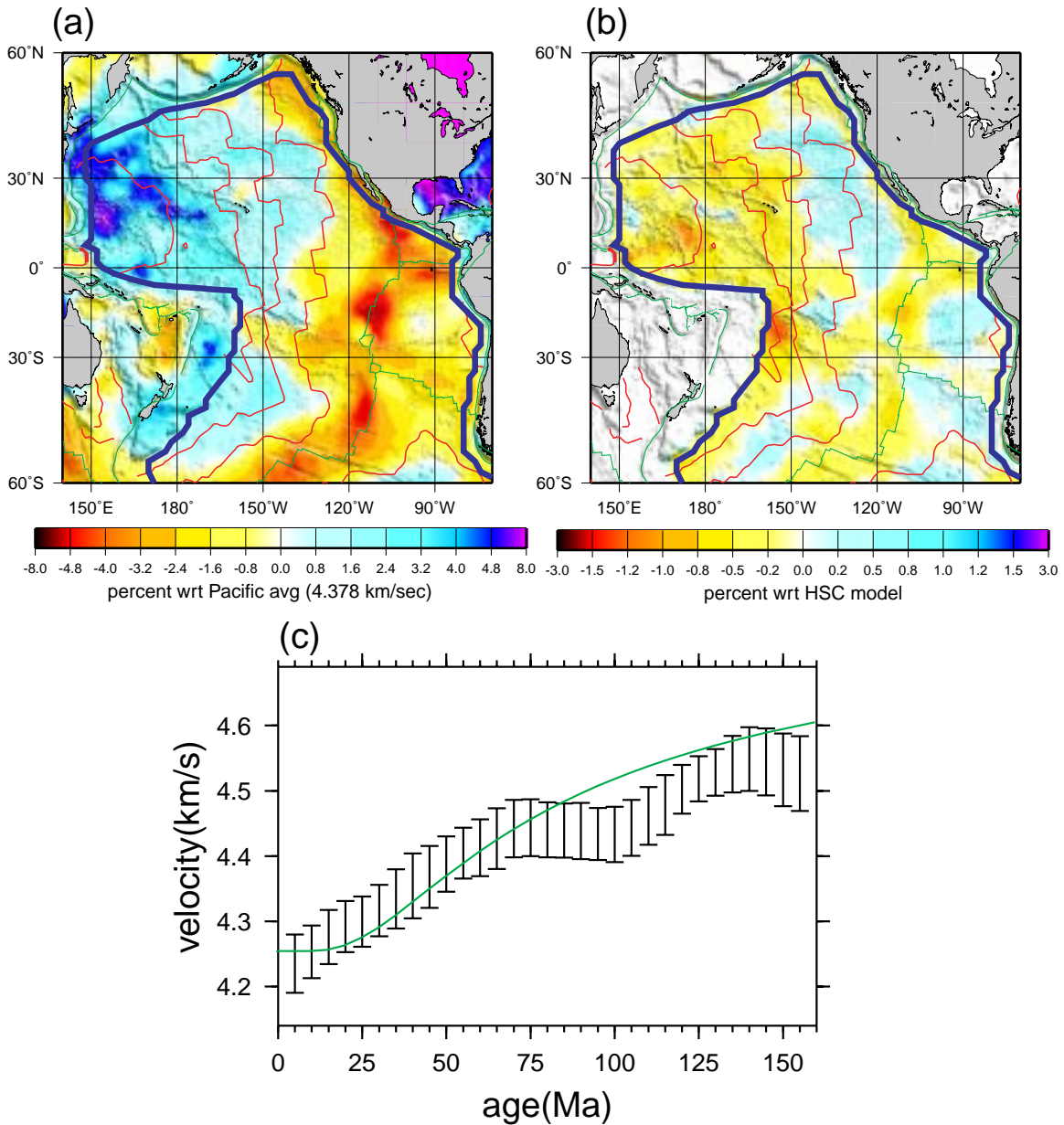


Figure 7: **Shear velocity structure of the Pacific upper mantle using the seismic parameterization and trend with lithospheric age.** (a) Shear velocity at 100 km depth, as a perturbation to the average at this depth across the Pacific (4.378 km/sec). The green lines denote plate boundaries, the red lines are isochrons of lithospheric age in increments of 35 Ma, and the blue contour encloses the region where there are lithospheric age estimates. (b) Shear velocity at 100 km depth presented as a perturbation to the prediction from the HSC model. (c) Shear velocity, averaged in 5 Ma lithospheric age bins across the Pacific, is plotted versus lithospheric age at 100 km depth. Error bars represent the standard deviation within each age range. The continuous green line is the predictions from the HSC model shifted vertically the same amount as in the analogous figure in the main text: -30 m/s. This figure should be contrasted with the model derived using the temperature parameterization, Figure 3a-c in the revised paper.

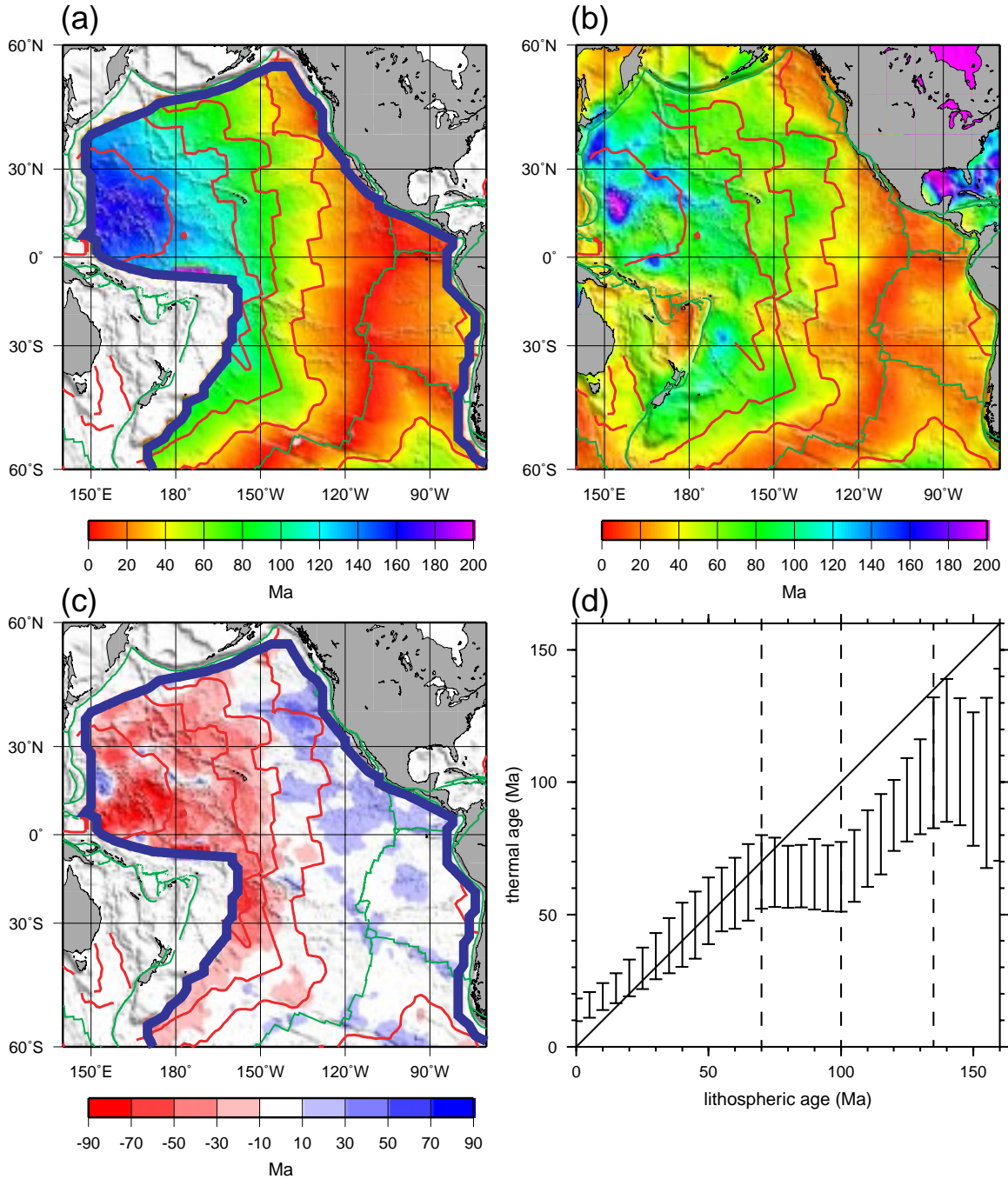


Figure 8: **Thermal age and age trend determined with the seismic parameterization.** (a) Lithospheric age in Ma, presented as a reference. (b) Apparent thermal age, τ , estimated with the seismic parameterization. (c) Difference between the lithospheric age and the apparent thermal age. Reds denote that the apparent thermal age is younger than the lithospheric age. (d) Comparison between apparent thermal age and lithospheric age. Apparent thermal age is averaged in 5 Ma lithospheric age bins across the Pacific and error bars represent the standard deviation within each age range. Contrast with Figure 4a-d in the revised paper, based on the thermal parameterization.

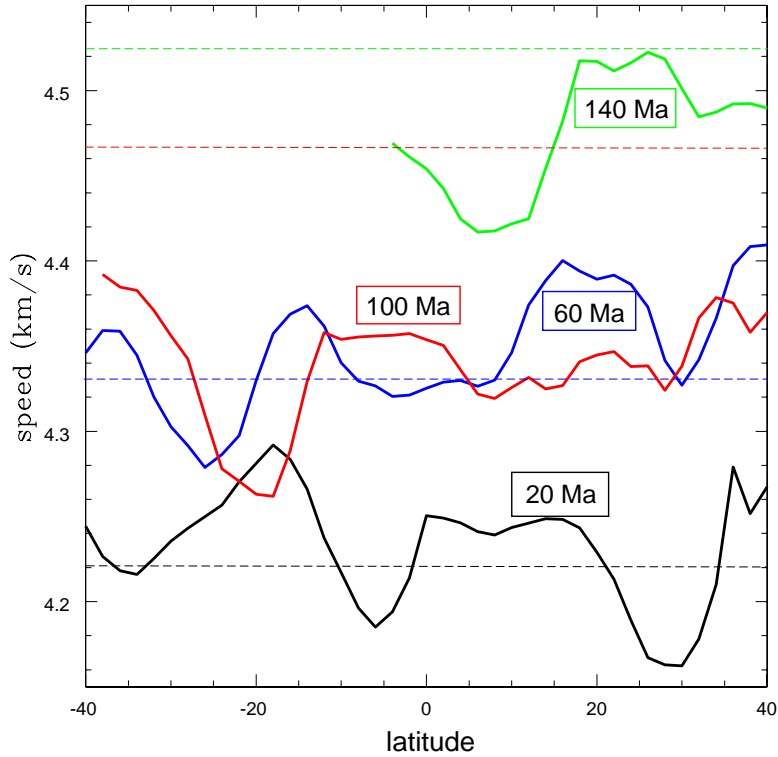


Figure 9: Shear velocity at 100 km depth plotted as a function of latitude (parallel to isochrons) in the Pacific. (Solid Lines) Observed velocities for four age ranges: (black) 20 ± 5 Ma, (blue) 60 ± 5 Ma, (red) 100 ± 5 Ma, (green) 140 ± 5 Ma. (Dashed Horizontal Lines) Predictions from the HSC model color coded the same as the observations; from Figure 3c in the paper.